Polymer 49 (2008) 3957–3964

Contents lists available at ScienceDirect

Polymer

journal homepage: www.elsevier.com/locate/polymer

pH and salt responsive poly(*N*,*N*-dimethylaminoethyl methacrylate) cylindrical brushes and their quaternized derivatives

Youyong Xu [a], Sreenath Bolisetty [b], Markus Drechsler [a], Bing Fang [a], Jiayin Yuan [a], Matthias Ballauff [b], Axel H.E. Müller [a,*]

[a] Makromolekulare Chemie II, Bayreuther Zentrum für Kolloide und Grenzflächen, Universität Bayreuth, D-95440 Bayreuth, Germany
[b] Physikalische Chemie I, Bayreuther Zentrum für Kolloide und Grenzflächen, Universität Bayreuth, D-95440 Bayreuth, Germany

ARTICLE INFO

Article history:
Received 6 May 2008
Received in revised form 22 June 2008
Accepted 27 June 2008
Available online 5 July 2008

Keywords:
PDMAEMA
Polyelectrolytes
Clindrical polymer brushes

ABSTRACT

We present the synthesis and characterization of poly(*N*,*N*-dimethylaminoethyl methacrylate) (PDMAEMA) cylindrical brushes, their pH responsiveness, and the corresponding quaternized analog, poly{[2-(methacryloyloxy)ethyl] trimethylammonium iodide} (PMETAI) brushes. PDMAEMA brushes were prepared by atom transfer radical polymerization (ATRP) using the grafting-from strategy. Initiating efficiencies of the ATRP processes were determined by cleaving the side-chains and gel permeation chromatography (GPC) analysis. Due to the slow initiation and steric hindrance, the initiating efficiency is only around 50%. The PDMAEMA brushes show worm-like structures and pH responsiveness, as proven by dynamic light scattering (DLS), atomic force microscopy (AFM), and cryogenic transmission electron microscopy (cryo-TEM) measurements. Strong cationic polyelectrolyte PMETAI brushes were produced by quaternization of the PDMAEMA brushes. AFM and cryo-TEM images showed similar worm-like morphologies for the PMETAI brushes. The PMETAI brushes collapsed in solution with high concentration of monovalent salt, as proven by DLS and AFM results.

1. Introduction

With the rapid development of nano-science and nanotechnology, scientists' attention has been shifting from the preparation of various nanostructures and nano-materials to manipulable nano-devices [1,2]. Although researchers have long been successful in the microscopic motors, actuators, or sensors, the same concept in the nanometer scale has met great challenges due to the special properties of nano-objects.

In recent years, it became obvious that polymers can play an important role in building smart and controllable nano-objects owing to their natural advantages [3,4]. Firstly, the size of the polymer chains ranges in the nanometer scale. Secondly, polymers show diversified topologies like linear, star-like, dendritic, comb-shaped and crosslinked structures. Moreover, they can also self-assemble into different structures. Thirdly, because of their vast possibilities of functionalities, polymer can respond to different external or internal stimuli, such as pH, solvent, ions, temperature, radiation, electric or magnetic field [5].

Among polymers of different structures, cylindrical polymer brushes (CPBs) have drawn increasing attention for their potential as single-molecular responsive nano-objects. When the grafting density of polymer chains to a much longer linear chain is high enough, a cylindrical polymer brush is formed [6–9]. Because of the anisotropic nature and the worm-like structure, cylindrical brushes demonstrate special solution and bulk properties [10]. So far, three different strategies have been developed for the preparation of CPBs: grafting-onto [11], grafting-from [12,13] and grafting-through [7]. Every strategy has its own advantages and disadvantages. Different controlled/living polymerization techniques have also been applied to prepare well-defined CPBs: atom transfer radical polymerization (ATRP) [12,14,15], nitroxide mediated radical polymerization (NMP) [16,17], ring-opening polymerization (ROP) [18] and ring-opening metathesis polymerization (ROMP) [19].

There are already several examples of using CPBs as responsive nano-objects. Schmidt et al. showed that poly(*N*-isopropylacrylamide) (PNIPAAm) polymer brushes can transform from worm-like structures into spheres when the temperature is higher than the lower critical soluble temperature (LCST) [20]. Similar brushes with different backbone or side chains were also reported by McCarley et al. [21] and Matyjaszewski et al. [22]. Sheiko et al. [23] and Möller et al. [24] reported the conformational transition of cylindrical polymer brushes on a surface due to lateral pressure stimuli. Matyjaszewski et al. successfully prepared photo-tunable temperature responsive core–shell type cylindrical brushes [25].

* Corresponding author. Tel.: +49 921 55 3399; fax: +49 921 55 3393.
E-mail address: Axel.Mueller@uni-bayreuth.de (A.H.E. Müller).

0032-3861/$ – see front matter © 2008 Elsevier Ltd. All rights reserved.
doi:10.1016/j.polymer.2008.06.051

Polyelectrolytes are macromolecules carrying covalently bound anions or cationic groups with counterions providing electroneutrality [26,27]. Due to the Coulombic interactions they demonstrate special solution properties, which are strongly influenced by the type and concentration of salt in aqueous solution [28]. For weak poly-acids and -bases the pH value is another important parameter since it controls the ionization degree. Inspired by these special features of polyelectrolytes, the corresponding cylindrical polymer brushes may display totally different responsiveness compared to uncharged cylindrical brushes, which could be used for building smart single-molecular nano-objects. Although there are already several examples of polyelectrolyte cylindrical polymer brushes [29–32], most of the research was concentrated on the synthesis work. Few were conducted on the responsiveness and the transition of the polyelectrolyte cylindrical brushes.

Herein, we describe the synthesis of poly(*N*,*N*-dimethylaminoethyl methacrylate) (PDMAEMA) cylindrical brushes and their quaternized salts, poly{[2-(methacryloyloxy)ethyl] trimethylammonium iodide} (PMETAI) brushes. Previously, our group has reported on the multi-responsive solution properties of PDMAEMA linear and star polymers and their quaternized derivatives [33–35]. Due to the weak polyelectrolyte nature of the PDMAEMA, the corresponding cylindrical polymer brushes are expected to show different properties. Matyjaszewski et al. showed the temperature responsiveness of the PDMAEMA brushes at various concentrations in solution [36]. In this study, we will demonstrate the response of this type of brushes on pH and the concentration of monovalent salt. A detailed study with added di- and trivalent salts will be published elsewhere. The responsiveness of the PDMAEMA and PMETAI brushes could be potentially applied in nano-scale sensor systems or nano-actuator systems [37].

2. Experimental section

2.1. Materials

CuCl (97%, Aldrich) was purified by stirring with acetic acid overnight. After filtration, it was washed with ethanol and diethyl ether and then dried in vacuum oven. $CuCl_2$ (99%, Acros) was used without purification. 2-Dimethylaminoethyl methacrylate (98%, Merck) was purified by passing through basic alumina columns before polymerizations. *N*,*N*,*N*′,*N*″,*N*‴,*N*‴-hexamethyltriethylenetetraamine (HMTETA, Aldrich) was distilled before use. The synthesis of the macroinitiator poly(2-(2-bromoisobutyryloxy)ethyl methacrylate) (PBIEM) ($DP_n = 1500$, PDI = 1.08) by anionic polymerization was reported previously [15]. Methyl iodide was purchased from Aldrich and was used as received. All other solvents and chemicals were used as received. Regenerated cellulose membranes were used for the dialysis (ZelluTrans with MWCO = 4000–6000 Da from Roth, Karlsruhe, and Spectra/Pore 7 with MWCO = 1000 Da).

2.2. Polymerizations

All polymerizations were carried out in round-bottom flasks sealed with rubber septa. A typical example of the synthesis of PDMAEMA cylindrical brushes is described as follows: PBIEM (55.8 mg, 0.2 mmol of initiating α-bromoester groups) and HMTETA (46.1 mg, 0.2 mmol) were dissolved in anisole (31.4 g) in a round-bottom flask and stirred overnight to assure the complete dissolution of the high molecular weight macroinitiator. Then the monomer DMAEMA (15.7 g, 0.1 mol) was injected via a syringe and stirred for 15 min. $CuCl_2$ (5.4 mg, 0.04 mmol) was added, followed by Argon purging for 5 min. $CuCl_2$ was dissolved and the color became brown. Then CuCl (19.8 mg, 0.2 mmol) was added and the flask was purged with argon for 15 min. About 0.5 mL of solution was taken out with an argon-purged syringe as an initial sample for conversion measurement by ^{1}H NMR. The round-bottom flask was then inserted into a water bath at room temperature (25 °C). HMTETA was injected by argon-purged syringe to start the reaction. The solution immediately turned green. Small amounts of samples were taken out at intervals to check the monomer conversion by ^{1}H NMR. After 12.5 h, the reaction solution became viscous and was stopped by opening to the air. Final conversion determined by ^{1}H NMR reached 6.5%. THF was added to dilute the solution. After passing through a basic alumina column, the solution was concentrated by a rotary evaporator. Afterwards, it was precipitated into cold *n*-hexane to remove the residual monomer and other impurities. Then the polymer was re-dissolved in certain amount of dioxane. A part of the solution was subjected to freeze-drying and the other part was further diluted by dioxane and dialyzed against pure dioxane for 7 days. After the dialysis, a part of the dioxane solution was dialyzed against water for 7 days to switch the solvent from dioxane to water.

2.3. Synthesis of poly{[2-(methacryloyloxy)ethyl] trimethylammonium iodide} cylindrical brushes

To quaternize the obtained PDMAEMA brushes, the polymer was dissolved in dioxane. Methyl iodide was added at room temperature at a molar ratio of 2 compared to amino groups. After around 20 min, the solution became turbid. Stirring was continued for 2 days to ensure the full reaction. Then dioxane was decanted and the polymer was washed several times with diethyl ether. Afterwards, the quaternized polymers were dissolved in water and dialyzed against pure water for one week. Finally, it was freeze-dried to get white powders.

2.4. Cleavage of the side chains from the PDMAEMA brushes

The cleavage of the side chains from the quaternized PDMAEMA brushes was carried out by alkaline hydrolysis. One typical reaction is described as follows: 100 mg of quaternized PDMAEMA brushes and about 10 ml of concentrated NaOH (18 M) aqueous solution were put into a PE vial and heated for 10 days at 90 °C. After 1 h at 90 °C, some more drops of water were added to dissolve some suspending polymers. A dark brown precipitate was observed after the reaction and the smell of amine is also quite strong. The mixture was then cooled down and the supernatant solution was removed by syringe to separate it from the precipitate. Concentrated HCl solution was added to the solution to tune the pH to around 4. This

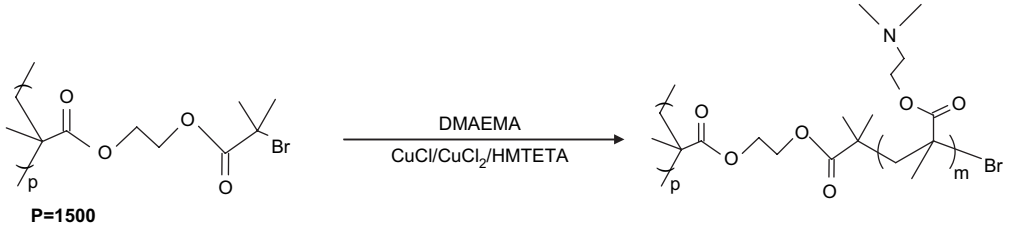

Scheme 1. Synthetic strategy of the PDMAEMA cylindrical brushes.

Table 1
Synthesis, molecular characterization and light scattering measurements of PDMAEMA brushes[a]

Sample	B1	B2
Conversion[b]	6.5%	8.0%
$DP_{sc,calc}$[c]	32	40
$10^{-5}M_{n,app,GPC}$[d]	6.26	6.85
PDI_{app}[d]	1.33	1.35
10^{-6} $M_{n,calc}$[e]	7.95	9.84
10^{-6} $M_{w,SLS}$[f]	8.64	12.40
R_h,[g] nm (PDI)	25 (0.126)	32 (0.165)

[a] ATRP at 25 °C with 33.3 wt% DMAEMA concentration in anisole and constant ratio of $s_0/[I]_0/[CuCl]_0/[CuCl_2]_0/[HMTETA] = 500:1:1:0.2:1$. $DP_{n,backbone} = 1500$.
[b] Monomer conversion determined by ^1H NMR.
[c] Calculated DP of side-chains, $DP_{sc,calc} = ([M]_0/[I]_0) \times$ conversion.
[d] Apparent values determined by conventional GPC with NMP as the eluent and PS calibration.
[e] Calculated from monomer conversion; $M_{n,calc} = (157 \times DP_{sc,calc} + 279) \times DP_{n,backbone}$.
[f] Determined by SLS in dioxane.
[g] Hydrodynamic radius and polydispersity measured by DLS in dioxane.

solution was freeze-dried and redissolved in water. Dialysis was carried out against pure water by using regenerated membranes (Millipore SpectraPore 7 MWCO 1000) over 3 days. In order to ensure the full protonation of the final product, poly(methacrylic acid) (PMAA), a small amount of HCl was added before freeze-drying the solution. ^1H NMR measurement in D_2O was performed to check the conversion of the ester cleavage. Aqueous GPC was used to check the molecular weight of the final PMAA product with a PMAA calibration.

2.5. Characterization

^1H NMR was measured on a Bruker AC-250 instrument at room temperature with $CDCl_3$ or D_2O as the solvent.

The apparent molecular weights of the PDMAEMA brushes were characterized by conventional gel permeation chromatography (GPC) using 0.05 M solution of LiBr in 2-*N*-methylpyrrolidone (NMP) as eluent at a flow rate of 1.0 mL/min at room temperature. PSS GRAM columns (300 mm × 8 mm, 7 μm): 10^3, 10^2 Å (PSS, Mainz, Germany) were thermostated at 70 °C. An RI detector and a UV detector ($\lambda = 270$ nm) were used. Polystyrene standards (PSS, Mainz) with narrow molecular weight distribution were used to calibrate the columns, and methyl benzoate was used as the internal standard.

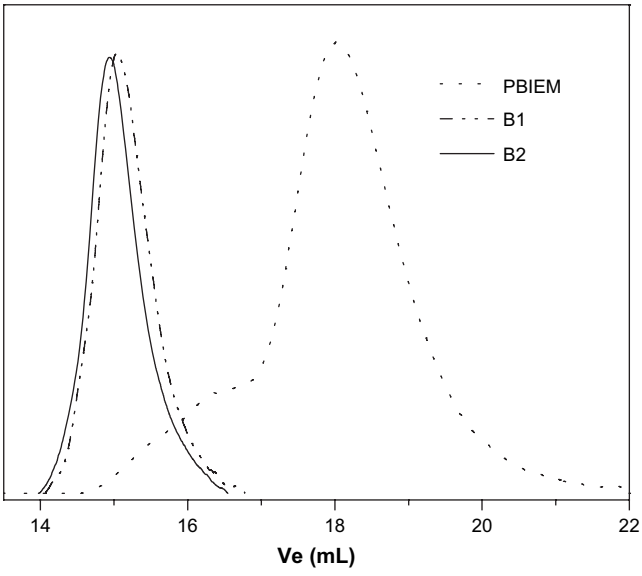

Fig. 1. GPC curves of the PDMAEMA brushes in NMP (RI detection).

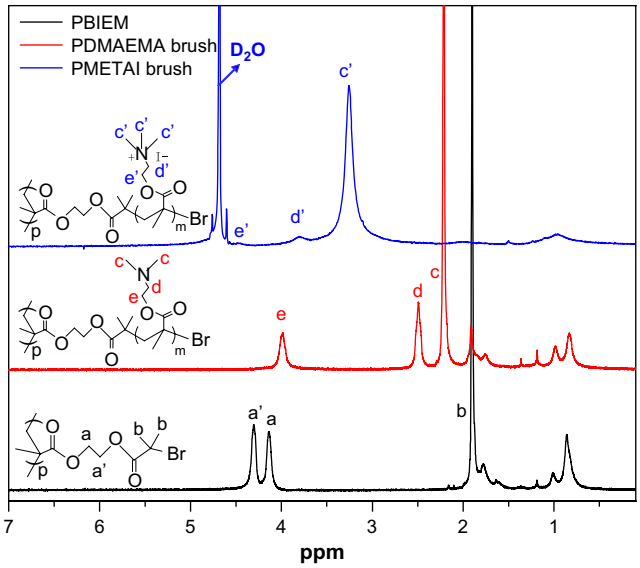

Fig. 2. ^1H NMR of PBIEM, PDMAEMA brush and PMETAI brush.

An *aqueous GPC* (internal standard, ethylene glycol; additives: 0.1 M NaN_3, 0.01 M NaH_2PO_4) was applied to obtain the molecular weight of PMAA (PMAA standards, PSS, Mainz). Column set: two 8 mm PL Aquagel–OH columns (mixed and 30 Å), operated at 35 °C and RI detection.

2.6. Static light scattering

Static light scattering (SLS) was measured on a Sofica goniometer using a He–Ne laser ($\lambda = 632.8$ nm). Prior to the light scattering measurements, the sample solutions were filtered 3 times by using Millipore Teflon filters with a pore size of 0.45 μm. Five concentrations of the PLMA cylindrical brush solutions in dioxane were measured at angles in the range from 30° to 150°. The weight-average molecular weight, M_w, of the PDMAEMA brushes was obtained by the analysis of the Zimm-plots. The refractive index increment of the PDMAEMA cylindrical brushes in dioxane solution at 25 °C was measured to be $dn/dc = 0.0543$ mL/g using a PSS DnDc-2010/620 differential refractometer.

2.7. Dynamic light scattering

Dynamic light scattering (DLS) was carried out on an ALV DLS/SLS-SP 5022F compact goniometer system with an ALV 5000/E correlator and a He–Ne laser ($\lambda = 632.8$ nm) at an angle of 90°. For the PDMAEMA brush solutions in dioxane, the sample solutions were filtered 3 times by using Millipore Teflon filters with a pore size of 0.45 μm before the light scattering measurements. For the water solution of PDMAEMA brushes at different pH and quaternized brushes at different salt concentration, the sample solutions were filtered by Millipore nylon filters with pore size of 0.45 μm. CONTIN analyses were performed for the measured intensity correlation functions. Apparent hydrodynamic radii, R_h, of the cylindrical brushes were calculated according to the Strokes–Einstein equation [38]. All the measurements were carried out at 25 °C. For the measurement of quaternized brushes in salt solutions, the change of viscosity of the aqueous solutions was taken into account. For salt concentrations higher than 0.2 M the obtained hydrodynamic radius was divided by the relative viscosity [33].

2.8. Atomic force microscopy

Atomic force microscopy (AFM) measurements were performed on a Digital Instruments Dimension 3100 microscope operated in

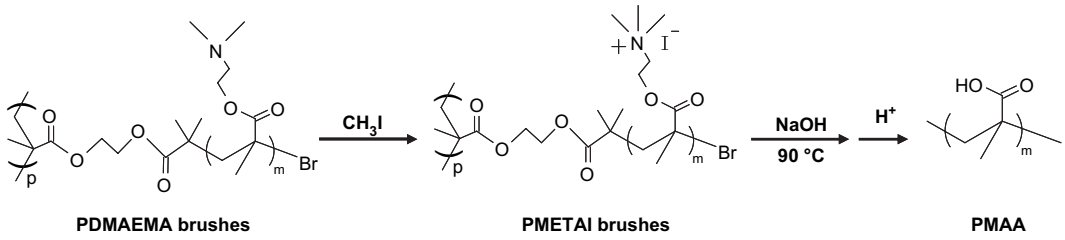

Scheme 2. Procedure for the quaternization and cleavage reactions.

tapping mode. The micro-cantilever used for the AFM measurements were from Olympus with resonant frequency between 284.3 kHz and 386.0 kHz, and spring constant ranging from 35.9 to 92.0 N/m. For the PDMAEMA brushes in THF solution, the samples were prepared by dip coating from very dilute (0.01 g/L) THF solutions of PDMAEMA brushes onto freshly cleaved mica surfaces. For the measurement of the quaternized brushes in water, very dilute aqueous solutions (0.02 g/L) were prepared and were spin-coated on freshly cleaved mica.

2.9. Cryogenic transmission electron microscopy

For cryogenic transmission electron microscopy (cryo-TEM) studies of PDMAEMA brushes and the quaternized brushes, a drop of the sample (aqueous solution, concentration around 0.01 g/L) was put on an untreated bare copper TEM grid (600 mesh, Science Services, München, Germany), where most of the liquid was removed with blotting paper, leaving a thin film stretched over the grid holes. The specimens were instantly shock vitrified by rapid immersion into liquid ethane and cooled to approximately 90 K by liquid nitrogen in a temperature-controlled freezing unit (Zeiss Cryobox, Zeiss NTS GmbH, Oberkochen, Germany). The temperature was monitored and kept constant in the chamber during all the sample preparation steps. After the sample is frozen, it was inserted into a cryo-transfer holder (CT3500, Gatan, München, Germany) and transferred to a Zeiss EM922 EFTEM. Examinations were carried out at temperatures around 90 K at an acceleration voltage of 200 kV. Zero-loss filtered images ($\Delta E = 0$ eV) were taken under reduced dose conditions (100–1000 electrons/nm^2). All images were registered digitally by a bottom-mounted CCD camera system (Ultrascan 1000, Gatan) combined and processed with a digital imaging processing system (Gatan Digital Micrograph 3.10 for GMS 1.5).

3. Results and discussion

3.1. Syntheses of PDMAEMA brushes

The PDMAEMA cylindrical brushes were prepared by the combination of anionic polymerization and ATRP using the grafting-from strategy. The synthesis of the backbone of the brushes by anionic polymerization with DP = 1500 and a very low polydispersity was reported previously by our group [15]. Scheme 1 shows the synthetic strategy of the PDMAEMA cylindrical brushes.

It has been known that the initiating efficiencies of grafting from the backbone for the synthesis of cylindrical brushes are limited due to the steric hindrance [39,40]. In order to obtain relatively densely grafted cylindrical brushes, some points have to be taken into account. Matyjaszewski et al. have shown that reducing the monomer concentration and increasing the copper amount enhances the grafting efficiency [40]. It is also known that initiation of methacrylates is more efficient when bromine is exchanged to chlorine by the use of CuCl [41]. Using HMTETA as the ligand and anisole as the solvent has proved to work well for the ATRP of linear DMAEMA polymers [42]. Thus, for our system, we chose CuCl as the catalyst, HMTETA as the ligand and anisole as the solvent. Since the monomer DMAEMA is quite reactive, we added 20% $CuCl_2$ to the system to lower the rate of polymerization. Quite low monomer concentrations were used with the weight ratio of DMAEMA to anisole 1:2. Temperature also plays a very important role. Whereas crosslinked polymer was obtained at 70 °C, soluble polymers were achieved at room temperature. Table 1 lists the results of the polymerizations. It shows relatively low polydispersity for the brushes, considering the extremely high molecular weight. The molecular weights determined by conventional GPC were not true values since the compact structure of the brushes is not comparable with that of the linear polystyrene standards. However, the calculated molecular weights do not deviate much from the true molecular weight determined by static light scattering in dioxane, indicating that the synthesis of the PDMAEMA brushes was successful.

Although conventional GPC cannot give true molecular weights of the brushes, it still can show the difference of the eluent volume changes between the brushes and the macroinitiator. Fig. 1 shows the GPC eluent curves of the PDMAEMA brushes. They both demonstrate monomodal distributions, indicating good control of the ATRP grafting reactions. There is a coupling peak for the macroinitiator PBIEM, which has been reported before [15]. Since the coupling peak covers only a small part of the PBIEM polymer, and the polydispersity of the macroinitiator is very low, it does not influence the final brushes too much.

Solutions of PDMAEMA brushes in dioxane were also subjected to dynamic light scattering analysis. The plots of the decay rates versus the square of the scattering vector are linear and lead to the apparent hydrodynamic radii given in Table 1. The CONTIN plots of both brushes (at 90° scattering angle) are monomodal and the polydispersities, as determined by the cumulant method are below 0.2, demonstrating the narrow distribution of the PDMAEMA brushes.

Fig. 2 shows the ^{1}H NMR spectra of the PDMAEMA brushes. The two peaks at 4.1 and 4.3 ppm (a, a′), are assigned to the methylene protons between two ester groups in the PBIEM macroinitiator. When the PDMAEMA cylindrical brushes are formed, peaks a and a′ disappear, while distinctive peaks from the dimethylaminoethyl groups appear: methyl protons (c, 2.2 ppm) connected to the amino group, methylene protons (d, 2.5 ppm) neighboring to the amino groups, and the other methylene protons (e, 3.95 ppm) connected to the ester groups. Thus, the ^{1}H NMR spectra indicate the successful grafting of PDMAEMA from the PBIEM backbones.

Table 2
GPC results of PMAA arms obtained after cleaving and initiating efficiencies

Sample	PDMAEMA brush	PMETAI brush[a]	10^3 $M_{n,GPC}$[b]	PDI[b]	$DP_{sc,calc}$[c]	$DP_{sc,GPC}$[d]	f[e]
PMAA1	B1	Q1	5.6	1.38	32	65	50%
PMAA2	B2	Q2	7.1	1.38	40	82	49%

[a] Q1 and Q2 are the quaternized brushes corresponding to the PDMAEMA brushes B1 and B2.
[b] Determined by water GPC using PMAA calibration.
[c] From Table 1.
[d] $M_{n,GPC}/86$.
[e] Initiating efficiencies, $f = DP_{sc,calc}/DP_{sc,GPC}$.

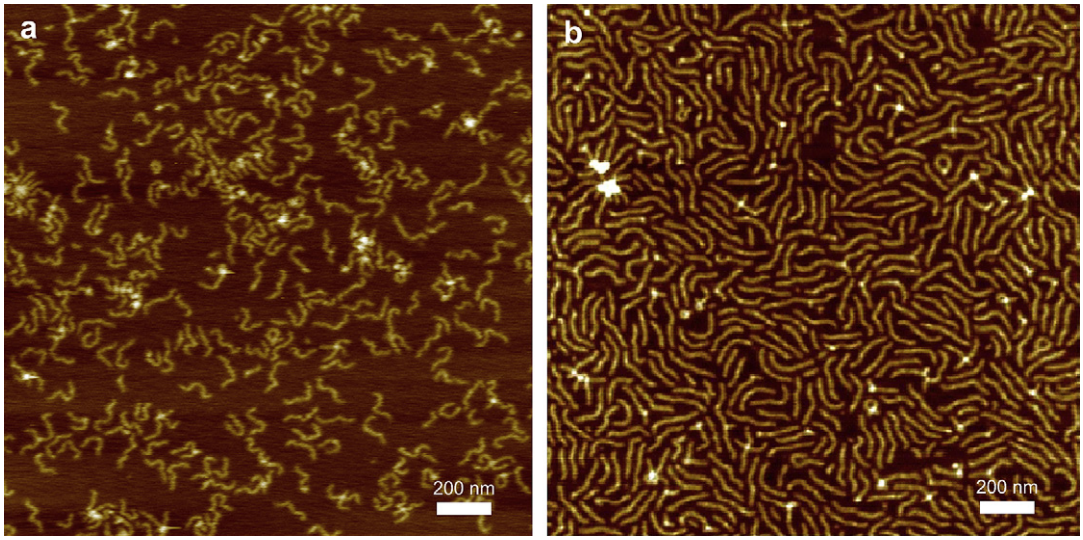

Fig. 3. AFM height images of PDMAEMA brushes B1 (a) and B2 (b) obtained by dip coating from 0.01 g/L THF solutions onto mica. The *Z* ranges for images (a) and (b) are 4 nm and 5 nm, respectively.

3.2. Quaternization and grafting densities

The grafting-from strategy does not always provide full initiator efficiency, leading to lower than expected grafting densities. Since the grafting density influences the length, flexibility and other characteristics of the CPBs, its knowledge is important. The ester bonds connecting the side-chains to the backbone are used for the cleavage of the side-chains by a strong base. Because of the LCST behavior of PDMAEMA in aqueous solution at pH > 7, it is not convenient to cleave the PDMAEMA brushes' side chains in basic solutions. Thus, the brushes were quaternized by methyl iodide to their salt form, PMETAI, and subjected to a strong base and heating. This treatment not only cleaves the ester linkage between the side-chains and the backbone, but also the ester groups in the monomer units. Scheme 2 shows the procedures of the quaternization and cleavage reactions.

From Fig. 2, we can compare the ^{1}H NMR spectra of the PDMAEMA brushes and the quaternized PMETAI brushes. After quaternization, the distinct peaks from the methylaminoethyl groups all shift to higher chemical shift: methyl groups connected to the ammoniums (c′, 3.2 ppm), methylene groups adjacent to the ammoniums (d′, 3.75 ppm) and the other methylene groups linking to the ester groups (weak peak e′, 4.4 ppm). It is also found that there are no peaks left at the original peak positions (c, d, e), which indicates quantitative quaternization of the PDMAEMA brushes. Thus, strong cationic polyelectrolyte PMETAI brushes are obtained.

The cleavage of arms from PMETAI star polymers has already been reported by our group [33]. The similar procedure was used to detach the side-chains from the PMETAI brushes. The final product, poly(methacrylic acid) (PMAA), was separated and purified for ^{1}H NMR and aqueous GPC analyses. ^{1}H NMR and water GPC eluent curves of the PMAA cleaved from quaternized B2 sample are shown in the Supplementary data.

The GPC results and calculated initiating efficiencies are listed in Table 2. According to the GPC results, the cleaved PMAA shows monomodal distribution. However, the polydispersity is relatively high (1.38), which is close to the value 1.33 expected for slow initiation [43]. Since DMAEMA is a quite active monomer and there is remarkable steric hindrance on the backbone, the propagation rate of DMAEMA chains is expected to be much higher than that of initiation. In both brushes the initiating efficiencies are ca. 50%, irrespective of halogen exchange and lower monomer concentration used. Nevertheless, the grafting-from strategy is effective for the preparation of cylindrical brushes despite its inevitable relatively low grafting density.

Thus, both brushes consist of 1500 monomer units in the backbone and carry ca. 750 side chains of $DP_n = 65$ and 82 for brushes B1 and B2, respectively.

3.3. AFM imaging of the PDMAEMA brushes

The morphology of the PDMAEMA brushes is shown by AFM. Fig. 3 displays the AFM height images of sample B1 and B2, dip-coated on the freshly cleaved mica surface from THF solution. From Fig. 3, we see that the B1 brushes are quite curved while B2 brushes are more stretched, indicating a higher persistence length. Nevertheless, their average lengths are both around 170 nm, which is ca. 45% of the contour length of the totally stretched backbone length ($L_c = 1500 \times 0.25$ nm $= 375$ nm), probably due to the low grafting density and the not too long side-chains (65 and 82 monomer units, respectively).

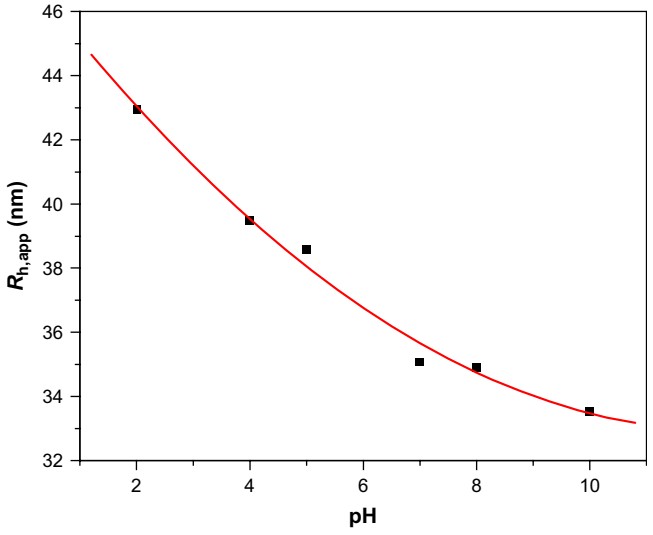

Fig. 4. Hydrodynamic radii of PDMAEMA brush B2 in 0.2 g/L aqueous solution at different pH values.

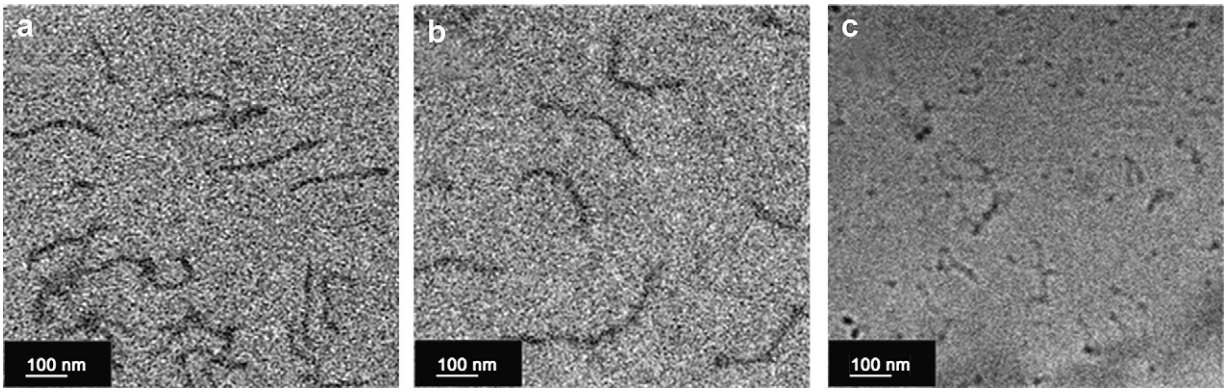

Fig. 5. Cryo-TEM images of PDMAEMA brushes in vitrified 0.01 g/L aqueous solution at (a) pH 2, (b) pH 7 and (c) pH 10.

3.4. pH responsiveness of PDMAEMA brushes

Since PDMAEMA is a weak cationic polyelectrolyte, its degree of ionization depends on pH. The apparent pK_b value (p$K_b = 14 - $pH at 50% ionization) for stars with a large number of arms is around 8 [35] and we expect the same behaviour here. In the case of CPBs, a change in ionization is expected to induce structural changes. DLS measurements for the brushes at different pH values were carried out in water at a scattering angle of 90°. Fig. 4 shows the hydrodynamic radii of the PDMAEMA brush B2 at different pH values. All measurements were performed in the absence of salt at very low concentration (0.2 g/L) to avoid intermolecular aggregation at high pH values. An obvious pH dependence of the apparent hydrodynamic radii is observed. Whereas R_h at pH 10 is close to the one obtained in dioxane, the values increase by 10 nm between pH 10 and pH 2, which is explained by the stretching of the PDMAEMA brushes at low pH (high ionization) and collapse at high pH.

In order to see the true morphological changes of the PDMAEMA brushes, cryo-TEM measurements were performed at pH 2, pH 7 and pH 10 in the absence of salt. Fig. 5 displays the cryo-TEM images of PDMAEMA brushes in aqueous solution at a concentration as low as 0.01 g/L. It is seen that the length of the PDMAEMA brushes at pH 7 is around 180 nm, which is slightly higher than that measured by AFM. In AFM, the brushes are tightly adsorbed at the mica surface and this surface effect must be taken into account when measuring the size of the brushes. In the cryo-TEM system, the solutions were vitrified in an extremely short time and the images reveal almost the true situations of the brushes in the solution state. At pH 7, the PDMAEMA brushes take worm-like structures and some of them are quite curved. At pH 2, most of the brushes are protonated and ionized, and they show more stretched morphologies. More remarkably, at pH 10, the brushes are strongly contracted with an average length around 110 nm, which is attributed to a collapse of the non-ionized PDMAEMA side chains.

3.5. Morphology of PMETAI cylindrical brushes

By quaternization with methyl iodide the weak polyelectrolyte PDMAEMA brushes are converted to strong polyelectrolyte brushes, that is, all side chains carry charges irrespective of the pH in the system. From the ^{1}H NMR spectra in Fig. 2, the successful conversion was proven. Fig. 6 shows typical AFM and cryo-TEM images of PMETAI brush Q2. On mica surface, the PMETAI brushes show a quite curved structure, which again is attributed to the strong interaction of the cationic brushes with negatively charged mica substrate. However, the worm-like structure of the charged CPBs is immediately obvious. The length of the PMETAI brushes is around 180 nm, similar to that of the PDMAEMA brushes on surface or in solution.

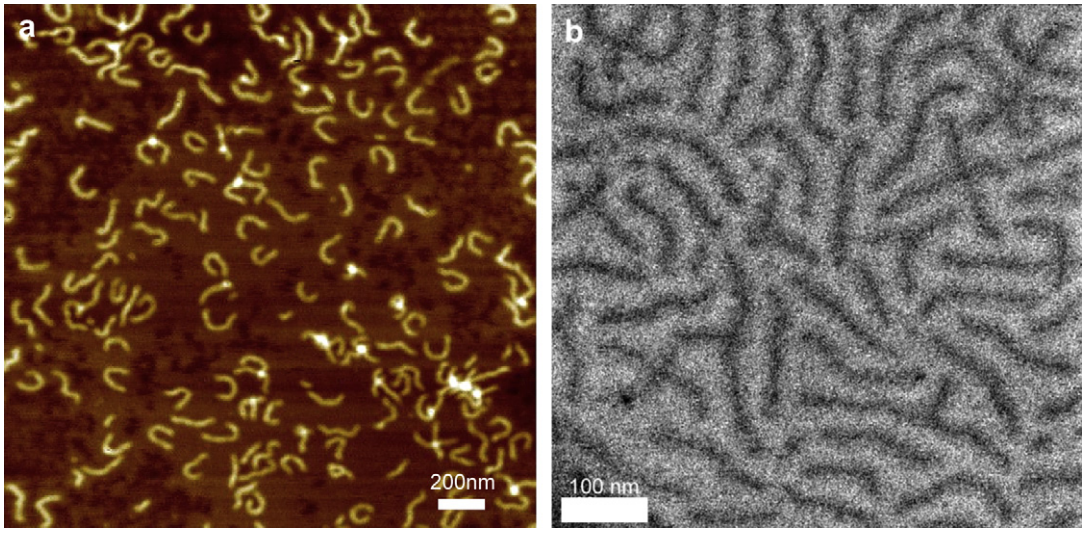

Fig. 6. (a) AFM height image (*Z* range 7 nm) and (b) cryo-TEM image of PMETAI brushes.

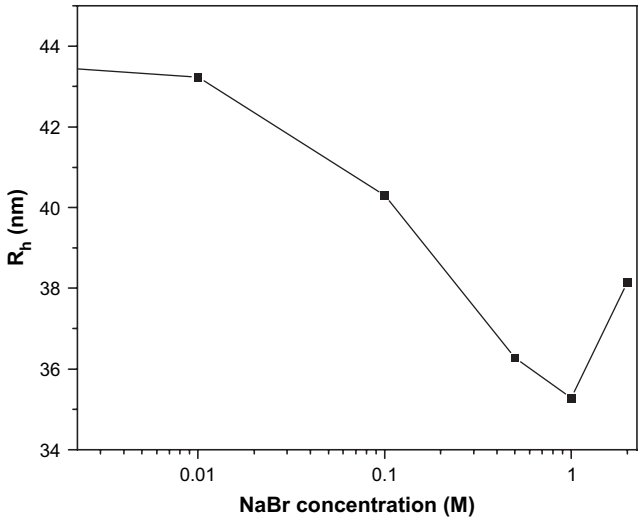

Fig. 7. Apparent hydrodynamic radii of the PMETAI brushes as a function of NaBr concentration.

3.6. Effect of monovalent salt

Due to the strong Coulombic repulsion of the charged chains, the strong polyelectrolyte PMETAI brush assumes a rather elongated conformation. Although, due to Manning condensation, the majority of counterions are confined in the brush [44–47], the charge density is still high enough to considerably stretch the brush. Addition of salt to the solution will screen the electrostatic interaction within the polyelectrolyte. Thus, the stretching of the polyelectrolyte chains should be diminished and the conformation should be more collapsed. Fig. 7 shows the change of the hydrodynamic radii of the PMETAI Q2 brush with increasing NaBr concentration. There is a remarkable decrease of the apparent R_h when salt is added. Increasing the NaBr concentration from 0 M to 1 M leads to a decrease of 8 nm in R_h. This marked change of the overall shape has already been studied for planar and spherical polyelectrolyte brushes [29,48]. However, Schmidt et al. [29] reported no significant change of the R_g and R_h for quaternized polyvinylpyridine (PVP) brushes when the concentration of added salt was increased to 0.1 M. Here we performed the DLS measurements at a wider range of salt concentrations (up to 2 M of NaBr). Whereas the apparent hydrodynamic radius is equal to the one for the non-quaternized brush at pH = 2, we indeed find a pronounced decrease of R_h at high salt concentration. The reasons for this discrepancy are not obvious and may be traced back to a difference in grafting density, which is higher for the PVP brushes synthesized by the polymerization of PVP macromonomers.

When the salt concentration is higher than 1 M, the apparent R_h increases again, as has also been found for the spherical polymer brushes [49]. As already pointed out there, bromide ions may have specific interactions with cationic polyelectrolyte chains. Hence, a solution of NaBr of sufficient concentration will lead to an adsorption of bromine ions onto the polyelectrolyte chains which is followed by a re-swelling of the brushes.

The collapse of the PMETAI brushes at high salt concentration can directly be visualized by AFM. Fig. 8 shows the AFM height image of the PMETAI brushes on mica, spin-coated from its 0.5 M NaBr solution. It is clearly seen that most of the brushes show an ellipsoid-like conformation and the length of the brushes is less than 100 nm, which is much lower than that shown in Fig. 6.

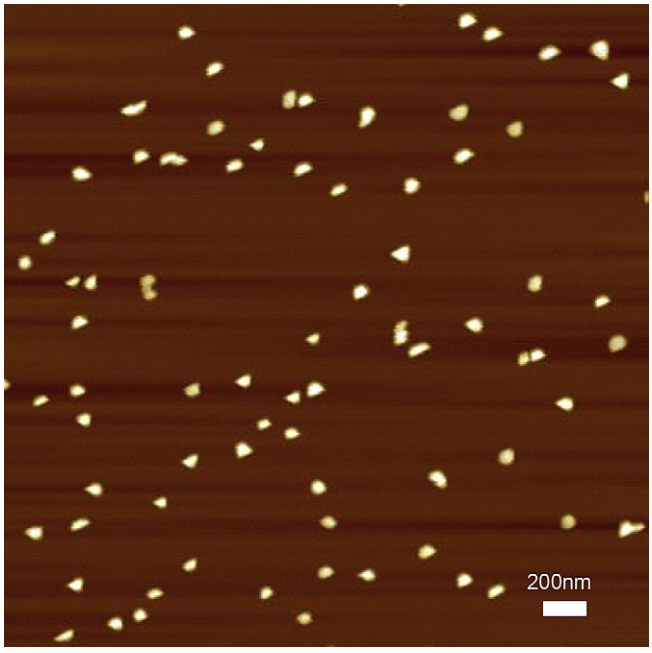

Fig. 8. AFM height image of PMETAI brushes on mica spin-coated from 0.5 M NaBr solution. *Z* range is 12 nm.

4. Conclusions

We have demonstrated the successful preparation of PDMAEMA cylindrical brushes using the grafting-from strategy by ATRP. The initiating efficiencies of the ATRP processes were determined by cleaving the side-chains and GPC analysis. The initiating efficiency is around 50%, probably due to slow initiation caused by steric hindrance. DLS, SLS and AFM measurements clearly show the worm-like structure of the PDMAEMA brushes in solution. The brushes also show pH responsiveness as proven by DLS and cryo-TEM at different pH values. ^{1}H NMR confirms the successful quaternization of PDMAEMA brushes to form strong cationic polyelectrolyte PMETAI brushes. The PMETAI brushes collapse in solution with high concentration of monovalent salt, as were evidenced by DLS and AFM.

Acknowledgement

Financial support from *Deutsche Forschungsgemeinschaft* (DFG) within SFB 481 is acknowledged. The authors want to express their gratitude to Sabine Wunder and Markus Hund for their help with the GPC and AFM measurements, respectively. Helpful discussions with Felix Plamper and Pierre Millard are appreciated.

Appendix. Supplementary data

Supplementary data associated with this article can be found in the online version, at doi:10.1016/j.polymer.2008.06.051.

References

[1] Schwarz JA, Contescu CI, Putyera K. Dekker encyclopedia of nanoscience and nanotechnology, 5 volume set. Boca Raton: CRC Press; 2004.
[2] Whitesides GM. Small 2005;1:172–9.
[3] Liu T, Burger C, Chu B. Prog Polym Sci 2002;28:5–26.
[4] Rodriguez-Hernandez J, Checot F, Gnanou Y, Lecommandoux S. Prog Polym Sci 2005;30:691–724.
[5] Minko S. Responsive polymer materials: design and applications. Oxford: Blackwell Publishing Ltd.; 2006.
[6] Tsukahara Y, Mizuno K, Segawa A, Yamashita Y. Macromolecules 1989;22:1546–52.
[7] Dziezok P, Sheiko SS, Fischer K, Schmidt M, Möller M. Angew Chem Int Ed 1997;36:2812–5.

[8] Pyun J, Kowalewski T, Matyjaszewski K. Macromol Rapid Commun 2003;24:1043–59.
[9] Zhang M, Müller AHE. J Polym Sci Part A Polym Chem 2005;43:3461–81.
[10] Bolisetty S, Airaud C, Xu Y, Müller AHE, Harnau L, Rosenfeldt S, et al. Phys Rev E 2007;75. Article no. 040803.
[11] Gao H, Matyjaszewski K. J Am Chem Soc 2007;129:6633–9.
[12] Beers KL, Gaynor SG, Matyjaszewski K, Sheiko SS, Möller M. Macromolecules 1998;31:9413–5.
[13] Cheng G, Böker A, Zhang M, Krausch G, Müller AHE. Macromolecules 2001;34:6883–8.
[14] Börner HG, Beers K, Matyjaszewski K, Sheiko SS, Möller M. Macromolecules 2001;34:4375–83.
[15] Zhang M, Breiner T, Mori H, Müller AHE. Polymer 2003;44:1449–58.
[16] Cheng C, Qi K, Khoshdel E, Wooley KL. J Am Chem Soc 2006;128:6808–9.
[17] Cheng C, Qi K, Germack DS, Khoshdel E, Wooley KL. Adv Mater 2007;19:2830–5.
[18] Lee H, Jakubowski W, Matyjaszewski K, Yu S, Sheiko SS. Macromolecules 2006;39:4983–9.
[19] Cheng C, Khoshdel E, Wooley KL. Nano Lett 2006;6:1741–6.
[20] Li C, Gunari N, Fischer K, Janshoff A, Schmidt M. Angew Chem Int Ed 2004;43:1101–4.
[21] Balamurugan SS, Bantchev GB, Yang Y, McCarley RL. Angew Chem Int Ed 2005;44:4872–6.
[22] Yamamoto S-I, Pietrasik J, Matyjaszewski K. Macromolecules 2007;40:9348–53.
[23] Sun F, Sheiko SS, Möller M, Beers K, Matyjaszewski K. J Phys Chem A 2004;108:9682–6.
[24] Gallyamov MO, Tartsch B, Khokhlov AR, Sheiko SS, Boerner HG, Matyjaszewski K, et al. Chem–Eur J 2004;10:4599–605.
[25] Lee H-I, Pietrasik J, Matyjaszewski K. Macromolecules 2006;39:3914–20.
[26] Mandel M. Encyclopedia of polymer science and engineering, vol. 11; 1987. p. 739–829.
[27] Dautzenberg H, Jaeger W, Kötz J, Philipp B, Stscherbina D. Polyelectrolytes: formation, characterization and application. München: Hanser Verlag; 1994.
[28] Manning GS. J Chem Phys 1969;51:924.
[29] Rühe J, Ballauff M, Biesalski M, Dziezok P, Gröhn F, Johannsmann D, et al. Adv Polym Sci 2004;165:79–150.
[30] Lienkamp K, Noe L, Breniaux M-H, Lieberwirth I, Gröhn F, Wegner G. Macromolecules 2007;40:2486–502.
[31] Lienkamp K, Ruthard C, Lieser G, Berger R, Gröhn F, Wegner G. Macromol Chem Phys 2006;207:2050–65.
[32] Kroeger A, Belack J, Larsen A, Fytas G, Wegner G. Macromolecules 2006;39:7098–106.
[33] Plamper FA, Schmalz A, Penott-Chang E, Drechsler M, Jusufi A, Ballauff M, et al. Macromolecules 2007;40:5689–97.
[34] Plamper FA, Schmalz A, Ballauff M, Müller AHE. J Am Chem Soc 2007;129:14538–9.
[35] Plamper FA, Ruppel M, Schmalz A, Borisov O, Ballauff M, Müller AHE. Macromolecules 2007;40:8361–6.
[36] Pietrasik J, Sumerlin BS, Lee RY, Matyjaszewski K. Macromol Chem Phys 2007;208:30–6.
[37] Dai L. Intelligent macromolecules for smart devices: from materials synthesis to device applications. London: Springer-Verlag; 2003.
[38] Chu B. Laser light scattering – basic principles and practise. New York: Academic Press; 1991.
[39] Neugebauer D, Sumerlin BS, Matyjaszewski K, Goodhart B, Sheiko SS. Polymer 2004;45:8173–9.
[40] Sumerlin BS, Neugebauer D, Matyjaszewski K. Macromolecules 2005;38:702–8.
[41] Matyjaszewski K, Shipp DA, Wang J-L, Grimaud T, Patten TE. Macromolecules 1998;31:6836–40.
[42] Zhang X, Xia J, Matyjaszewski K. Macromolecules 1998;31:5167–9.
[43] Gold L. J Chem Phys 1958;28:91–9.
[44] Pincus P. Macromolecules 1991;24:2912–9.
[45] Borisov OV, Zhulina EB. Eur Phys J B 1998;4:205–17.
[46] Jusufi A, Likos CN, Löwen H. Phys Rev Lett 2002;88:018301.
[47] Jusufi A, Likos CN, Löwen H. J Chem Phys 2002;116:11011–27.
[48] Ballauff M. Prog Polym Sci 2007;32:1135–51.
[49] Mei Y, Ballauff M. Eur Phys J E 2005;16:341–9.